Galileo E5a/E5b and GPS L5 Acquisition Time Statistical Characterization and Application to Civil Aviation

Frederic Bastide, *ENAC/STNA/TeSA, France*

BIOGRAPHY

Frederic Bastide graduated as an electronics engineer at the ENAC in 2001, Toulouse. He is now a Ph.D student at the ENAC and is supported by the STNA (Service Technique de la Navigation Aérienne). Currently he carries out researches on DME/TACAN and JTIDS/MIDS signals impact on future GNSS receivers. He also spent 6 months at the Stanford GPS Lab in 2003 as an exchange researcher.

ABSTRACT

The initial task of a receiver is to acquire at least four satellites and then track them to compute a first fix. The acquisition process is a two-dimensional search both in time and frequency. Indeed neither the received code delay nor the carrier Doppler frequency are perfectly known and so must be searched. In the literature, only the mean acquisition time and its standard deviation can be found for acquisition strategies such as the classical single dwell or double dwell serial time search processes. However this characterization is not sufficient for applications such as civil aviation for which time to first fix requirements are paramount. Given RTCA MOPS 229, the acquisition process performance may be stated in terms of probability of success so statistical characterization of the acquisition time such as the probability density function (Pdf) or, equivalently, the cumulative density function (Cdf) are required. The effect of key parameters such as the signal quality, the dwell time or the number of available correlators on the acquisition performance has been assessed.

The future GPS L5 signal and GALILEO E5a and E5b signals are of particular interest for the civil aviation community. Indeed they will be broadcast in an ARNS band and are expected to increase accuracy, availability, integrity and continuity of service. The PRN spreading codes selected for these signals can be acquired directly using a traditional search scheme although a strategy combining both the data and pilot codes is shown to be more efficient as described in [1]. However E5a/L5 and E5b bands interfering environment is severe and mainly composed of pulsed signals transmitted by DME/TACAN and JTIDS/MIDS systems. They constitute a real threat causing large signal-to-noise ratio degradations especially at high altitude and so potentially jeopardize the compliance to the acquisition timing requirements. It is particularly true when the GNSS receiver experiences a power outage or brownout during en-route at FL 400 and must afterwards satisfy initial acquisition performance.

The aim of this paper is to present Monte Carlo simulation results enabling to estimate the acquisition time Pdf and Cdf for the classical single dwell serial time search process. The spreading codes for the considered signals are transmitted at high frequency (10.23 Mcps) causing possible high code Doppler frequencies as compared to GPS L1 C/A code for instance. The acquisition performance degradation, particularly for large dwell times, is quantified accordingly. These results are used to verify in which conditions the civil aviation requirements for initial acquisition can be satisfied.

INTRODUCTION

When a GNSS receiver is powered on, it does not always know perfectly its position, satellite positions and its time offset. So it has first to acquire GNSS signals. Signal acquisition means the search of the received code delay and Doppler frequency. Statistical characterization of the acquisition time is of particular interest for civil aviation since the initial acquisition process requirements can be stated in terms of probability of success. However, only the mean value and standard deviation for acquisition strategies, such as the single dwell time search, are available in publication [2]. There are no analytical expressions of the probability density functions that are required. Moreover, for future GPS L5 and Galileo E5a/E5b signals, the most challenging acquisition happens when the aircraft is flying at high altitude (FL 400) where many DME/TACAN beacon signals are received. In particular worst locations (hot-spots) over the US and Europe have been studied and the associated degradations computed. JTIMDS/MIDS system also brings additional degradation and if the receiver experiences a power outage at these locations, acquisition is not granted.

Hence, the purpose of the study presented in this paper it to estimate probability density functions for GPS L5 and Galileo E5a/E5b codes through Monte Carlo simulations. Statistical properties depend on the dwell time and the

number of available correlators. Degradation of acquisition performance due to the higher code Doppler frequency for high frequency code (i.e. 10.23 Mcps) as compared to L1 C/A code when the dwell time is large is assessed to ensure satisfaction of acquisition requirements.

The first part of this paper recalls the acquisition process when both data and pilot correlator outputs are used. Associated performance is also derived. Then simulations results regarding acquisition time distribution are presented in the second part. Eventually, the results are applied to the civil aviation requirements.

GPS L5 AND Galileo E5a/E5b ACQUISITON PROCESS

The acquisition process consists of a two-dimensional search both in time and in frequency. Indeed, because the user and satellite positions are not known, the received code phase must be searched. Also relative changes in user/satellite distances create a Doppler frequency that needs to be searched as well. Moreover uncertainty on time must be accounted for. There are different acquisition configurations such as the cold start where no a-priori information is available and so the entire PRN code and the full range of possible Doppler frequencies have to be explored. Another type is the warm start for which satellite almanac data, amongst other information, are available. This latter acquisition will be studied in subsequent sections.

The signal detection problem is based on a hypothesis test. Hypothesis H_1: the useful signal is present and H_0 it is not. A test statistic is computed and compared to a threshold. Generally the process is designed to match a given probability of false alarm *Pfa* but also to achieve a desired probability of detection *Pd* in the correct code/frequency bin.

A previous paper [1] has demonstrated the improvement brought by the combination of both data and pilot correlator output samples in the case of GPS L5-like signals. The improvement pertains to the probability of signal detection and the mean acquisition time as well. In this paper we assume future Galileo E5a and E5b signals are similar to GPS L5 signals and can therefore be modeled as two QPSK modulations carrying navigation data on the so called data channel and without any data on the pilot channel.

The signal *s(k)* entering the acquisition structure presented in Figure 1 has been first filtered, down-converted and sampled (quantization effect is neglected). Even if Neuman-Hoffman codes are implemented on GPS L5 they will not be considered in this study since they do not influence performance for our acquisition strategy. The generic expression of the considered signals is then

$$s(k) = \sqrt{C}.d(kT_S - \tau).c_{data,f}(kT_S - \tau).\cos(2\pi f_{IF} kT_S - \theta) + \sqrt{C}.c_{pilot,f}(kT_S - \tau).\sin(2\pi f_{IF} kT_S - \theta) + n(k)$$

where

- C is the total useful (data+pilot) received power at the antenna port
- $d(k)$ is the navigation message
- $c_{data,f}$ and $c_{pilot,f}$ are respectively the filtered versions of the data and pilot spreading codes c_{data} and c_{pilof}
- τ is the time-varying propagation delay
- f_{IF} is the final intermediate carrier frequency
- θ is the time-varying carrier phase
- n is the filtered Gaussian thermal noise

So as to search a single code/frequency bin, four elementary hardware correlators are required, two on each channel. The considered acquisition process structure is depicted in the next figure.

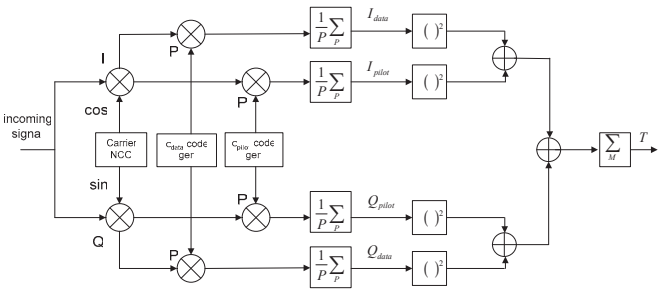

Figure 1 *Acquisition process structure*

where

- P is the number of cumulated samples so that the coherent integration time T_p equates $P.T_S$ with T_S the sampling period. The predetection bandwidth is $f_p=1/T_p$
- I_{data}, Q_{data}, I_{pilot} and Q_{pilot} are respectively the inphase/quadraphase correlator output samples of the data and pilot channels
- M is the number of non-coherent integrations

The decision test T is simply expressed as

$$T = \sum_{M} \left(I_{data}^2 + Q_{data}^2 + I_{pilot}^2 + Q_{pilot}^2 \right)$$

Neglecting cross-correlation between data/pilot spreading codes, correlator output samples (at the end of the coherent integration) may be modeled as follows:

$$I_{data}(k) = \sqrt{\frac{C}{4}}.D(k).\frac{\sin(\pi\Delta f T_P)}{\pi\Delta f T_P}.\cos(\varepsilon_\theta(k)).R_{data,f}(\varepsilon_\tau(k)) + n_{I,data}$$

$$Q_{data}(k) = \sqrt{\frac{C}{4}}.D(k).\frac{\sin(\pi\Delta f T_P)}{\pi\Delta f T_P}.\sin(\varepsilon_\theta(k)).R_{data,f}(\varepsilon_\tau(k)) + n_{Q,data}$$

$$I_{pilot}(k) = -\sqrt{\frac{C}{4}}.D(k).\frac{\sin(\pi\Delta f T_P)}{\pi\Delta f T_P}.\sin(\varepsilon_\theta(k)).R_{pilot,f}(\varepsilon_\tau(k)) + n_{I,pilot}$$

$$Q_{pilot}(k) = \sqrt{\frac{C}{4}}.D(k).\frac{\sin(\pi\Delta f T_P)}{\pi\Delta f T_P}.\cos(\varepsilon_\theta(k)).R_{pilot,f}(\varepsilon_\tau(k)) + n_{Q,pilot}$$

where

- $D(k)$ is the navigation data bit sign over the kth coherent integration
- Δf is the frequency offset between the received and the local carriers
- ε_θ is the phase offset between the received and the local carriers
- ε_τ is the phase offset between the received and the local codes
- $R_{data,f}$ and $R_{pilot,f}$ are respectively the data and pilot cross-correlations between the received codes, that are filtered, and the local ones

The last terms in each previous expression correspond to the thermal noise contribution. It can be shown [3] that these noise samples are centered and of power $\sigma_n^2 = \beta.N_0.f_p/4$. The noise power is reduced by a factor β due to the front-end filtering. The double-sided thermal noise power spectral density level is denoted N_0.

First of all, we assume the useful signal is not present (hypothesis H_0 associated to test T_0). It means that the currently searched code/frequency bin does not contain the true code phase and Doppler frequency. In this case, only thermal noise terms are present and if considered independent then T_0/σ_n^2 is a chi-square distribution with $4.M$ degrees of freedom. Usually the probability of false alarm is a given parameter and satisfies $Pfa = Pr[T_0 > Th]$ where Th is the threshold to be found. It is easily computed numerically using Matlab functions for instance. Classical Pfa values are 10^{-3} to 10^{-4}. A refinement may be brought by considering the effect of a cross-correlation peak due to a strong interfering GPS or Galileo satellite. It will be adopted in this study.

Once the threshold Th has been evaluated it is possible to compute the probability of detection in the correct code/frequency bin (hypothesis H_1 associated to test T_1). Indeed in this case, T_1/σ_n^2 becomes a non-central chi-square distribution with again $4.M$ degrees of freedom, the non-centrality parameter being

$$\lambda = \frac{2}{f_p}.\frac{C}{\beta.N_0}\left(\frac{\sin(\pi\Delta f T_P)}{\pi\Delta f T_P}\right)^2.\sum_{k=1}^{M} R_f^2(\varepsilon_\tau)$$

This expression has been obtained by assuming data and pilot cross-correlations are equal. This assumption is particularly valid for the correct bin because the computed values are located around the correlation peak. The code offset is deemed constant over the coherent integration time.

The probability of detection equates $Pd = Pr[T_1 > Th]$. Clearly the probability of detection depends on the predetection bandwidth f_p, the signal quality through the signal-to-noise density ratio C/N_0, the frequency offset Δf, the number M of non-coherent integrations and the code phase offset during each coherent integration.

It is well known that increasing the coherent integration time is more effective than increasing the number of non-coherent integrations. However, attention must be paid when selecting the former for GPS L5 and Galileo E5a/E5b. Indeed it can be shown [4] that a robust code/carrier acquisition process is obtained when the coherent integration time does not exceed the spreading code period of 1 ms. Indeed the presence of tiered codes such as Neumann-Hoffman codes may considerably degrade the acquisition performance if the frequency offset Δf is too large.

In this paper, we focus on the classical single dwell time search strategy. Its study is a good approach indeed if feasibility can be demonstrated in this case then more complex techniques will, of course, satisfy civil aviation requirements as well. Amongst more complex methods are the double dwell time search and those employing a Fast Fourier Transform. The principle of the single dwell time search is pretty simple and is fully described in [2]. The entire uncertainty region is swept until a hit (test statistic above the threshold) is observed. Then the receiver starts a verification mode that may consist of both a further integration and an entry into tracking loops. If t the signal is not present, it is a false alarm and the acquisition process resumes. The associated lost time is modelled as $K.M.T_p$ where K is called the penalty factor. If the verification mode succeeds then the search is completed and stops.

Holmes only indicates in [2] the closed form of the acquisition time mean value and standard deviation with and without residual Doppler. In the latter case, the mean acquisition time is approximated as follows:

$$\overline{T} \cong \frac{(2-Pd).(1+K.Pfa)}{2.Pd}.(q.M.T_p)$$

This expression is valid when the uncertainty region size q is very large ($q >> 1$). Moreover, when $K.(1+K.Pfa) << q$ then the acquisition time variance is approximated by

$$\sigma^2 \cong (M.T_p)^2.(1+K.Pfa)^2.q^2.\left(\frac{1}{12}-\frac{1}{Pd}+\frac{1}{Pd^2}\right)$$

When considering residual Doppler, the mean acquisition time approximation becomes

$$\overline{T} \cong \frac{(2-Pd).(1+K.Pfa)}{2.Pd.\left(\frac{\Delta T_c}{T_c}+M.T_p.\Delta f_{Dopp,code}+K.M.T_p.\Delta f_{Dopp,code}.Pfa\right)}.(q.M.T_p)$$

where

- $\Delta T_c/T_c$ is the search step in fraction of a chip (1/2 generally)
- $\Delta f_{Dopp,code}$ is the offset between the received and local code Doppler frequency expressed in chip

The standard deviation is

$$\sigma^2 \cong \frac{(M.T_p)^2.(1+K.Pfa)^2.N^2.\left(\frac{1}{12}-\frac{1}{Pd}+\frac{1}{P_d^2}\right)}{\left(\frac{\Delta T_c}{T_c}+M.T_p.\Delta f_{Dopp,code}+K.M.T_p.\Delta f_{Dopp,code}.Pfa\right)^2}$$

Holmes noticed the probability density function of the acquisition time is very difficult to obtain in a closed form. However, as further explained, this function is necessary to determine under which conditions civil aviation requirements for acquisition time can be met. The second part of this paper details how the probability density function has been estimated by simulations.

SIMULATION OF ACQUISITION TIME STATISTICAL CHARACTERISTICS

As explained in the previous section, we focused our study on the single dwell time serial search acquisition process. Before carrying out Monte Carlo simulations, it is necessary to define the parameters of the acquisition process and some characteristics of the search.

The uncertainty region size is specified by the initial uncertainties on the code delay, Doppler frequency and time. The size is also influenced by the search step size. For simulations, the initial correct code/frequency bin has been uniformly distributed over the uncertainty interval. We assumed a code search step of half a chip and a Doppler search increment of 500 Hz. Because the considered codes are 10230-chip long a probability of false alarm of 10^{-4} seems more appropriate. Indeed, there will be on average 1 false alarm if the search succeeds after a first sweeping. More false alarms are undesired since the time lost for each of them is of the order of a few seconds and so is not negligible. A cross-correlation peak is also accounted for when computing the Pfa. As proposed in [5] we considered a peak of 19 dBHz that would correspond to the case where cross-correlation occurs on both data and pilot codes simultaneously.

Regarding the probability of detection in the correct code/frequency bin, it is derived from the theory presented in the previous section. Once the threshold *Th* has been computed to achieve the given probability of false alarm, the probability of detection only depends on the non-centrality parameter. It depends, among other parameters, on the frequency offset Δf and the sum of the *M* cross-correlations.

First, let's define how the received and local code phases vary in time. The carrier Doppler frequency is due to the relative change in time of the radial distance between the receiver and the transmitting satellite. At the start of the dwell time and at the first order, the received code delay may be expressed in chip as follows:

$$\tau(t) = \tau_0 - f_{Dopp,code}.t$$

The initial delay at the beginning of a dwell time is denoted τ_0 and the code Doppler frequency $f_{Dopp,code}$. Note that this expression implicitly assumes the Doppler frequency is constant in time and equates:

$$f_{Dopp,code} = \frac{f_{Dopp,carrier}.f_{code}}{f_{carrier}}$$

Where the Doppler frequency of the received carrier is $f_{Dopp,\text{carrier}}$. Within the receiver the generated code phase may be expressed in the same way as:

$$\tau_{loc}(t) = \tau_{0,loc} - \frac{f_{Dopp,carrier,loc}.f_{code}}{f_{carrier}}t$$

The Doppler frequency of the local carrier is denoted $f_{Dopp,carrier,loc}$ and $\tau_{0,loc}$ is the applied delay when a dwell time starts. Of course there is an offset between the receiver and satellite times but it is accounted for in $f_{Dopp,carrier,loc}$ and $\tau_{0,loc}$. That is why there is the same time denoted *t* in both expressions. This initial delay is changed by the receiver by half-chip increments during the search, and $\tau_{0,loc}$ may take the following values in chip: 0, ½, 1, 3/2, 2 etc…So the code phase offset during a dwell time is

$$\varepsilon_\tau(t) = \tau(t) - \tau_{loc}(t) = (\tau_0 - \tau_{0,loc}) - \frac{\Delta f.f_{code}}{f_{carrier}}t$$

Where $\Delta f = f_{Dopp,carrier} - f_{Dopp,carrier,loc}$ is the residual frequency offset between the received and the local carriers. The code phase offset is composed of a constant part $\tau_0 - \tau_{0,loc}$ and a time-varying component: $(\Delta f.f_{code}/f_{carrier}).t$. The latter term may be null if the frequency offset is equal to zero but Δf could get as large as half the frequency search step. In a worst-case approach the maximum time-varying component must be considered.

In previous analysis [1], the offset ε_τ has always been assumed constant. If we consider the case of GPS L1 C/A code, the time-varying term is negligible. For instance for

a dwell time of 60 ms and a maximum frequency offset of 250 Hz (search step of 500 Hz) it only equates a hundredth of chip. However on L5, the variation is much larger because of the higher code frequency (10 times larger) and the lower carrier frequency. The ratio of the L5 code Doppler to the L1 C/A code's is about 14 and because larger dwell times are very likely on L5, it will result in significantly larger code phase offset variations, i.e. a quarter of chip after 115 ms (with a 250 Hz frequency offset). Next plot enables a comparison of the L1 and L5 code phase offset ε_τ variation as a function of time when constant components are equal and a 250 Hz Doppler frequency offset.

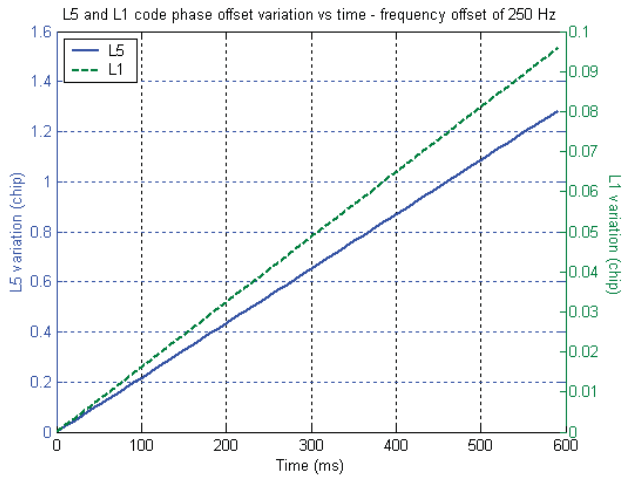

Figure 2 *L5 and L1 code phase offset variations as a function of time*

The case where the code phase offset is assumed constant (static case) will be treated first then the variation in time (dynamic case) will be integrated.

Constant code phase offset (static case)

Assume first the code phase offset is constant then the non centrality parameter becomes

$$\lambda = \frac{2.M}{f_p} \cdot \frac{C}{\beta . N_0} \cdot \left(\frac{\sin(\pi \Delta f T_P)}{\pi \Delta f T_P} \right)^2 . R_f^2(\varepsilon_\tau)$$

We assumed a code delay search step of ½ a chip then the worst case is when ε_τ= ¼ chip. The squared cross-correlation value at this offset is about -2.5 dB. Regarding the Doppler frequency search, in the correct bin, the worst case frequency offset is half the search step so +/- 250 Hz for 500 Hz steps. The squared sinus cardinal term equates in this case -0.9 dB. Moreover, for a 20 MHz double-sided bandwidth filter β=0.4 dB. Next plot shows the probability of detection for different numbers of non-coherent integrations as a function of the total C/N_0 that appears in the previous expression of the non-centrality parameter. The probability of false alarm is $Pfa=10^{-4}$ and a coherent integration time of 1 ms is assumed.

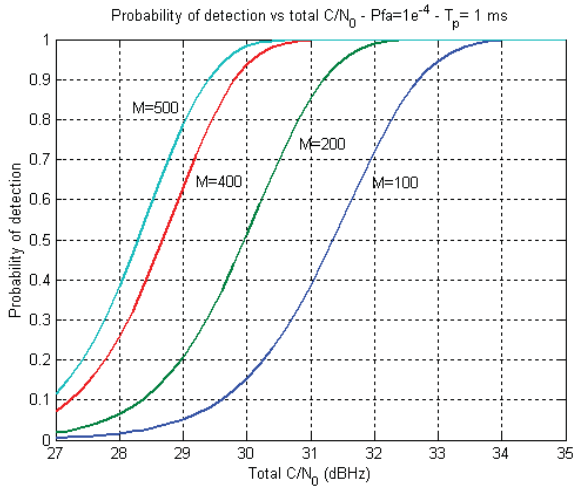

Figure 3 *Probability of detection as a function of the total C/N_0 for several numbers of non-coherent integrations – 1 ms coherent integration*

As will be demonstrated later, this approach does not correspond to the worst case. However when the dwell time is not too large (i.e. when the code phase offset variation is limited), the obtained performance are very close.

Future GNSS receivers will have a lot of available correlators. To fully exploit them, multiple correlators may be dedicated to the search of a single satellite signal. It allows the reduction of the acquisition time since multiple code/frequency bins may be explored at a time.

An example of the simulated acquisition time statistical characteristics is given in the following. Assume for this illustration the Doppler uncertainty is +/- 1 kHz so there are 4 frequency bins to search with a 500 Hz search step. If the uncertainty on the received code phase corresponds to the entire code length, then a maximum of 20460 code bins must be explored with half-chip steps for GPS L5 or Galileo E5a/E5b codes. Thus the uncertainty region size is q=4*20460=81840 bins. Now if the receiver has 160 hardware correlators then 40 of them may be dedicated to each Doppler bin. It also means that 10 code phase bins may be searched at once. We remind 4 elementary hardware correlators are required to search a single code/frequency bin. If the receiver wants to acquire "at any cost" the satellite signal then after a first unsuccessful sweeping of the whole uncertainty region it will restart the acquisition from the beginning. However if the receiver prefers to change of satellite it will have no impact on the statistical distribution of the acquisition time since restarting the search or changing the satellite is statistically equivalent assuming all satellites are received with the same signal-to-noise density ratio.

The uncertainty region in the considered example is illustrated on the next figure as well as the initial searched region, of size 40, that is filled with points.

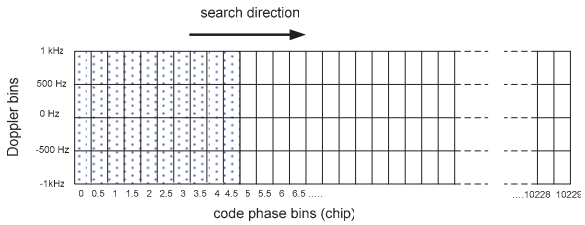

Figure 4 *Code/frequency uncertainty region and searched zone at the start of the acquisition process*

The first 40 code/frequency bins are searched during the dwell time and if no true hit is found then our strategy is to "jump" to the immediately adjacent region and so on until the signal is detected. This principle is illustrated on the next figure.

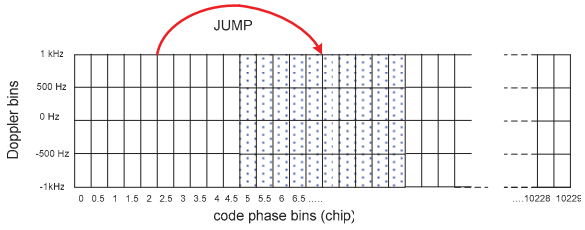

Figure 5 *Code/frequency uncertainty region and searched zone if no true hit has been found previously*

This acquisition strategy has been implemented through Monte Carlo simulations for three different C/N_0 (32.7 dBHz, 32.3 dBHz and 31.7 dBHz) implying as many probabilities of detection (0.9, 0.8 and 0.6 respectively). The dwell time was 100 ms and Figure 6 plots the obtained acquisition time probability density functions.

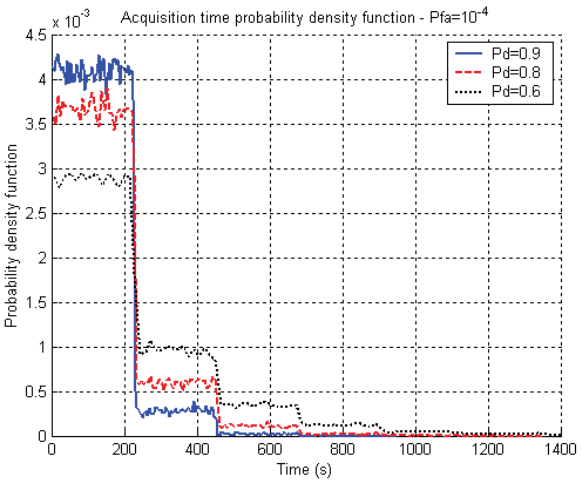

Figure 6 *Acquisition time probability density function for Pd=0.9, 0.8 and 0.6*

The first plateau that goes up to about 200 s corresponds to cases where the acquisition succeeded by exploring the uncertainty region only once. Indeed, according to our assumptions, the entire uncertainty region is explored by 81840/40=2046 "jumps" each lasting 100 ms so the total duration is about 200 s for a single sweeping. However because the probability of detection is not unity, there is some chance to find the correct code/frequency bin after additional sweepings represented by subsequent plateaus. Of course, the lower the probability of detection, the lower the first plateau and the higher the remaining ones. That is why the highest first plateau is for a probability of detection of 0.9 while the highest following ones are for Pd=0.6. The more correlators are available the smaller is the width of plateaus. An interesting property is that the distribution is pretty uniform on each plateau, which was to be expected. Figure 7 plots of the corresponding cumulative density functions.

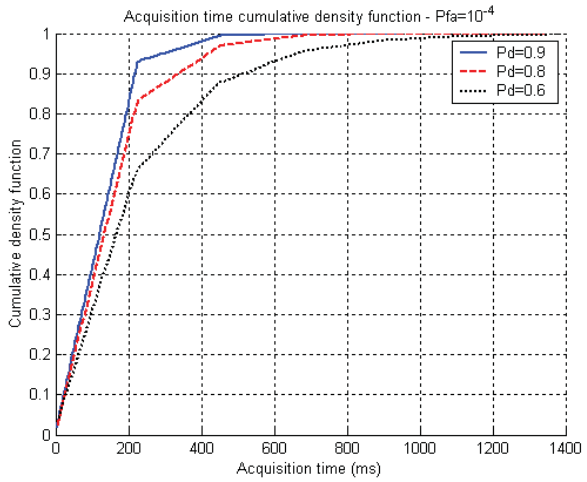

Figure 7 *Acquisition time cumulative density functions for Pd=0.9, 0.8 and 0.6*

The Cdfs are clearly composed of separate segments of different slopes corresponding to plateaus introduced previously. The largest slope for the first segment corresponds to Pd=0.9 which is consistent with Pdf plots. For subsequent segments, the largest slopes are for the lowest considered probability of detection Pd=0.6.

Then we compared the simulated mean values and standard deviations of acquisition times to the theoretical expressions indicated previously. The results are summarized in Table 1. Theoretical results are computed by dividing the initial uncertainty region size by 10.

Simulation and theoretical results agree very well validating our implementation of the single dwell time serial search process. Note that the same statistical results would have been found if, rather than searching the whole uncertainty region by blocks and then "jump", this region had been divided in 40 smaller separate uncertainty regions each explored repetitively by a single correlator

quadruplet. The reason is that the correct bin is uniformly distributed. If more correlators are available, the length of plateaus decreases accordingly. For instance if twice as much correlators are available so 320 instead of 160, the size of plateaus is divided by two while their heights are doubled.

Acquisition time	**Pd=0.9** simu/Holmes	**Pd=0.8** simu/Holmes	**Pd=0.6** simu/Holmes
mean value (s)	130.0/125.1	160.1/153.6	236.0/238.9
standard deviation (s)	92.7/93.1	131.3/128.8	222.8/223.8

Table 1 *Simulated and theoretical mean values and standard deviations of acquisitions time for the single dwell time serial search*

Time-varying code phase offset (dynamic case)

A more realistic approach, in a worst-case perspective, is to take into account the code phase offset change over time. The corresponding generic non-centrality parameter has been given previously in the paper and the only parameter remaining to be estimated is the sum of the M cross-correlations. Indeed the code phase offset changes from a coherent integration to the next so the M values are different. In the static case, we defined a worst case for the cross-correlation value (i.e. taken at an offset of half the code search step) and so we must do the same here. More precisely, we have to find conditions for which the sum is minimized and so will be the probability of detection. It can be shown the worst case depends on how much ε_τ changes during the dwell time and on its initial position at the start of the dwell time.

If the same acquisition strategy as the static case one is used then contiguous code bins are searched at once. We assume first that, during the dwell time, the code phase offset varies within bins that are part of the current searching block. We remind the receiver computes 1 ms cross-correlations for an initial local code phase corresponding to centers of code bins. The worst-case is when the variation is equally distributed over two or three bins depending on the dwell time. Figure 8 presents 2 cases, one for a variation larger than 2 code bins (dashed line) and the other one for a smaller variation (solid line). The plot is valid for either a positive or negative Doppler frequency and each dot correspond, accordingly, to either the start or the end of the code phase offset variation. Bins 1 and 4 will get very low cross-correlation as compared to bins 2 and 3. However the sum of the M cross-correlations (for a single code bin) is minimized because variation is equally distributed between bins 2 and 3 that will get the same sum. If the starting point of the variation displaced then either bin 2 or bin 3 will end up with higher sum improving performance.

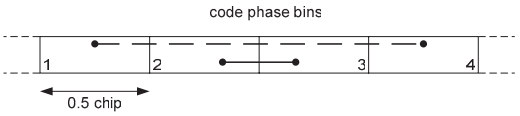

Figure 8 *Worst-case for the code phase offset variation*

An illustration of the evolution of the computed 1 ms cross-correlations in bins 1, 2 and 3 is given in Figure 9 for the case where the code phase offset varies from the center of bin 1 to the center of bin 4 (dashed line). It corresponds to a variation of 1.5 chips and assuming a frequency offset of 250 Hz, the corresponding dwell time is 1.5/250/10.23e6*1176.45e6=690 ms on L5/E5a and 708 ms on E5b. The incoming code has been filtered by a 20 MHz (double-sided bandwidth) filter. The deformation of the correlation peak due to the filtering is clear and the maximum value is 0.9.

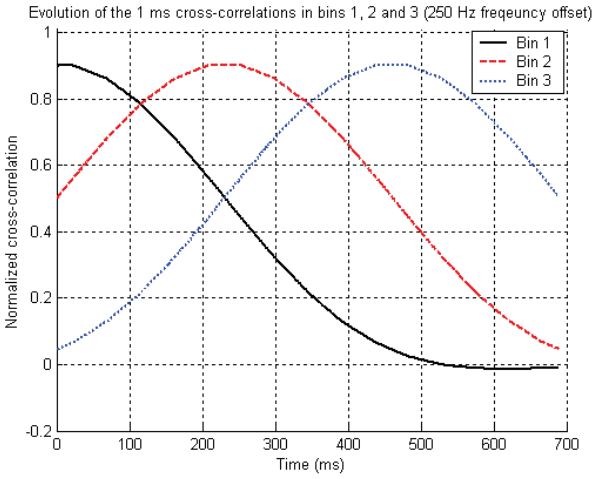

Figure 9 *Evolution of 1 ms cross-correlations computed in bins 1, 2 and 3 for a frequency offset of 250 Hz*

In bin 2 the cross-correlation value increases from 0.5 up to 0.9 when the code phase offset starts from the center of bin 1 to the center of bin 2. Then the value decreases to about 0.05 when the offset ends its variation at the center of bin 4. The sum of the $M=690$ squared cross-correlations is respectively 287 for bins 2 & 3 and and 152 for bin 1. In the static case this sum would be about 690*0.75= 517 (0.75 being the cross-correlation value at a quarter of chip offset). So non-centrality parameters are lower in the dynamic case implying lower probabilities of detection.

Performance degradation is now quantified in terms of the probability of detection. Next figure plots the probabilities of detection assuming a constant or time-varying code phase offset and various numbers of non coherent integrations.

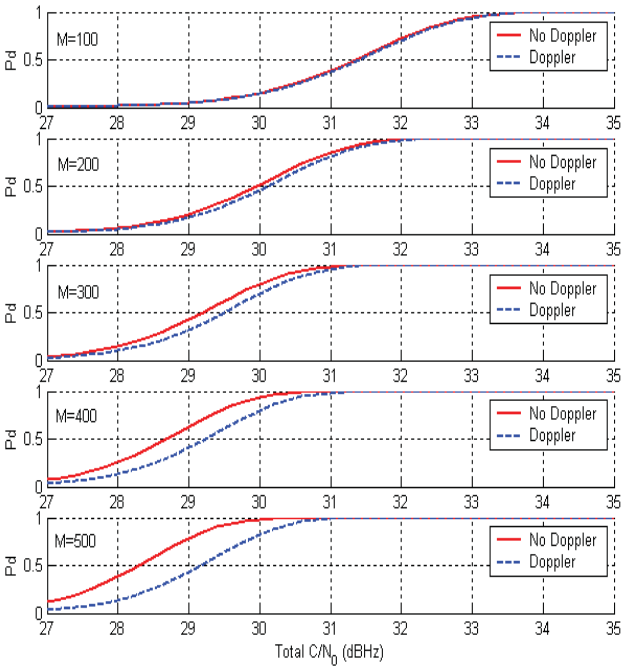

Figure 10 *Probability of detection with and without Doppler offset of 250 Hz and 100, 200, 300 ,400 and 500 non-coherent integrations*

Up to 200 ms the impact of the code phase offset variation during the dwell time is almost negligible. Indeed the probabilities of detection are very close. For larger dwell times the difference of achieved probability of detection gets higher, especially between 28 dBHz and 30 dBHz as the dwell time increases. In these conditions, acquisition performance is degraded.

Depending on the Doppler frequency offset sign the speed may be speed up or slow down. Indeed the code phase offset may get closer to the currently searched bins or may go away from them. This aspect is illustrated by the following simulation results. The two effects tend to counteract each other. For simulations, the frequency offset was chosen randomly with equal probability to have a positive or negative value.

Until now, it has been assumed that during the dwell time the code phase offset variation was always within currently searched code bins. However it may not be the case if, for instance, the variation is located at edges of the searching block. Now if the receiver jumps to the adjacent searching region then the signal could be missed. Note that of course there is a chance to detect the signal in this case but the probability of detection is very low. A way to prevent this event is to allow overlapping from a searching block to the adjacent one. The size of the overlapping should be the maximum code phase offset variation. For instance for a dwell time of 200 ms, the variation is about 0.4 chip so a 1-chip overlapping is necessary. This method causes a negligible reduction of the speed of search and its principle is illustrated in the next figure for an overlap of 2 code bins.

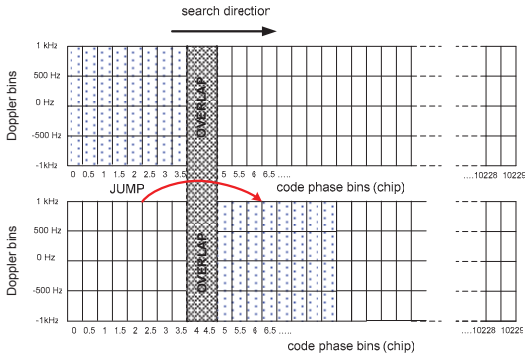

Figure 11 *Overlap strategy from a searching zone to the next one*

Then this acquisition strategy was simulated and compared to the static case. In this example, the dwell time is 400 ms and the C/N_0=30 dBHz. In the static case it corresponds to a probability of detection of 0.92 and 0.8 in the dynamic case. The obtained acquisition time probability density functions are indicated in Figure 12.

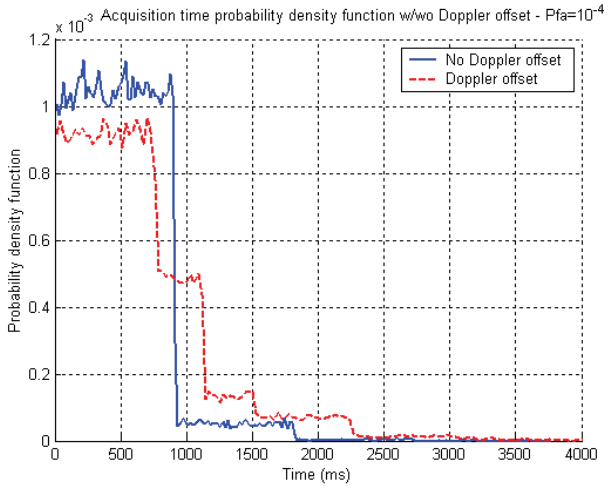

Figure 12 *Acquisition time probability density function in static and dynamic cases*

When comparing with Figure 6, the "dynamic" Pdf is not equivalent to the "static" Pdf assuming the same probability of detection (Pd=0.8 and dashed line in Figure 6). In fact it is an average between Pdfs for positive and negative Doppler frequency offsets. Figure 13 presents "positive" and "negative" Pdfs.

The first plateau of the "positive offset" case is shorter than the "negative case" one since the positive offset speeds up the search. For a negative offset, the searched is slow down because the correct code bin moves away from the searched region. The "positive" plateaus are higher accordingly.

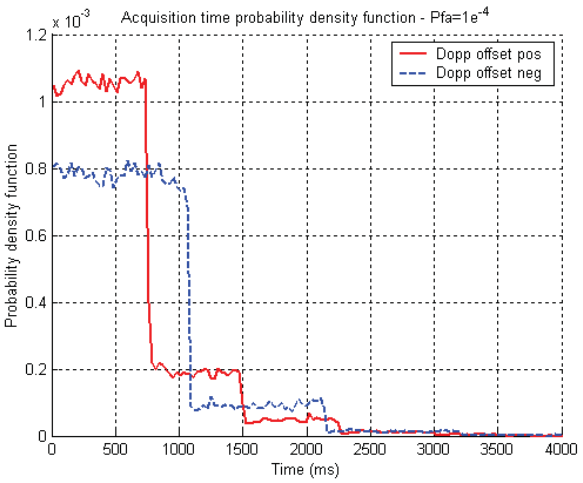

Figure 13 *Acquisition time probability density function with positive and negative Doppler offsets*

When averaging the two probability density functions, we get the mean Pdf plotted (solid plot) in Figure 14. It matches very well the Pdf obtained when the Doppler offset was either positive or negative with equal probability (see the dashed plot called "simulated function").

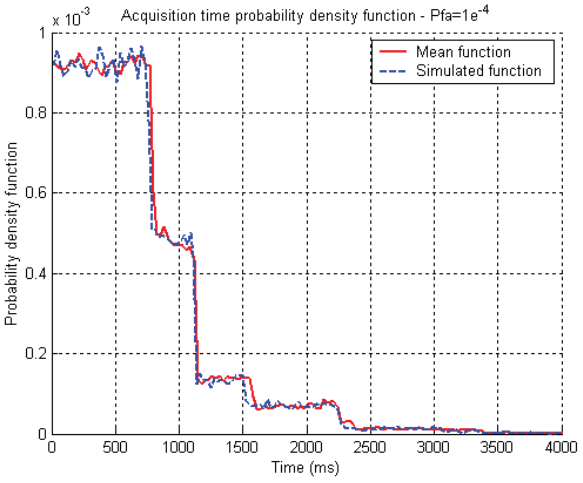

Figure 14 *Comparison of the mean acquisition time Pdf and the simulated one*

Holmes also indicates in [2] the mean value and standard deviation of the single dwell serial search acquisition time taking into account code Doppler offset. For the presented example, next table compares simulated and theoretical values. Last column presents results for simulations where the Doppler offset was either positive or negative with equal probability. In this case, theoretical values correspond to the mean of results obtained for the positive and negative cases. Theoretical results are computed by multiplying the search step $\Delta T_c/T_c$ by 10 that is the size of the searching block.

Doppler offset/ Acquisition time	**positive** simu/Holmes	**negative** simu/Holmes	**positive& negative** simu/Holmes
mean value (s)	577.4/523.0	721.7/743.2	650.3/633.1
standard deviation (s)	503.9/438.7	571.2/623.5	544.4/531.1

Table 2 *Simulated and theoretical mean values and standard deviations of the acquisition time for positive, negative and both Doppler offsets*

Again, simulated and theoretical values agree very well. Other simulations were also carried out confirming the consistency between our simulations and the theoretical model for the dynamic case.

APPLICATION TO CIVIL AVIATION

The RTCA MOPS DO 229 [6] specified the initial acquisition requirement as follows. The equipment shall be capable of acquiring satellites and determining a position without any initialization information, including time, position, and GPS and WAAS almanac data. In addition, with latitude and longitude initialized within 60 nautical miles, with time and date within 1 minute, with valid almanac data and unobstructed satellite visibility, and under interference conditions detailed in Appendix C of reference [6] and under the minimum signal conditions defined in Section 2.1.1.10 of reference [6], the time from application of power to the first valid position fix shall be less than 5 minutes. This requirement is applicable for an aircraft on the ground and also in flight after a power outage. The receiver is said to be in "warm start".

E5a/L5 and E5b bands interfering environment is severe because of DME/TACAN and JTIDS/MIDS pulsed systems that are the main contributors [7]. Large degradations of the effective signal-to-noise ratio are obtained at high altitude (FL 400) from where many DME/TACAN beacon signals are received. For instance over the European hot-spot, 121 beacons are "visible". Initial acquisition will be performed on ground by the aircraft before takeoff. However the GNSS receiver may experience a power outage on flight. If it happens at FL 400, there is a risk to not satisfy the initial acquisition requirements because of interference impact. Degradations have been estimated by simulations over the European and US hot-spots and so we know the available effective C/N_0 for acquisition. Our objective was to define the required parameters to get an acquisition threshold providing positive C/N_0 margins.

The time to first fix timing requirement can be apportioned as follows [8]:

- T_1=2.5 mn allocated to acquisition of first four satellites

- T_2=2.5 mn allocated to verification, tracking convergence, data demodulation…

This timing budget was obtained by first allocating the last 2.5 minutes. If ephemerides are demodulated twice for verification, it requires about 60 s. Moreover, tracking loops convergence and verification last a few seconds. Finally the allocated duration seems reasonable. RTCA WG 6 interpreted [9] the acquisition performance specified in DO 229 as a 95% value according to the Pass/Fail criteria determination for initial acquisition, see *2.5 Test Methods and Procedures* section [6]. It means that acquisition performance is met if the probability to acquire four satellites in less than 2.5 minutes is, at least, 0.95.

The initial code/Doppler uncertainties after a power outage have been estimated in [8]. It is assumed the receiver reads its clock offset and drift rate in a flash memory once power is restored. Thus the user oscillator drift that is generally the main uncertainty is greatly reduced. The uncertainty on Doppler was estimated to +/- 200 Hz (1 Doppler bin with a 500 Hz search step) and the uncertainty of code to the entire code length (2*10230 code bins for 0.5 chips search steps). A two-step strategy can be implemented. This strategy consists of the acquisition of a first satellite to reduce uncertainties and then the acquisition of 3 satellites to complete the position fix.

Once a first satellite has been acquired, remaining uncertainties for the acquisition of subsequent satellites are greatly reduced because the user clock uncertainty drops. In [8], they are estimated to a single Doppler bin and 4092*2=8184 code bins. So the first satellite is harder to acquire and there are about twice more bins to search. Thus it is proposed to allocate about twice as much time for the first satellite acquisition as for the subsequent ones. We must verify that:

$$Pb(Acquisition\ time\ 1^{st}\ sat \le 60s)$$

$$.Pb^3\left(Acquisition\ time\ subsequent\ sat < 30s\right) > 0.95$$

As explained earlier in the paper, there is no analytical expression of the acquisition time distribution; that is why we developed and ran simulations to estimate it and verify whether and how previous requirements can be met. Indeed, from the Pdf previous probabilities of acquisition can be easily deduced. As we have seen before, acquisition performance may be derived as a function of the number of receiver hardware correlators and dwell time.

First, we assumed to receive all satellite signals with the same C/N_0 corresponding to a worst-case (i.e. worst-case antenna gain). Another option is to select a first satellite with higher elevation and therefore a higher signal power level. This one may be asked to satisfy higher constraints such as a lower acquisition time hence relaxing constraints on subsequent satellites. In the following, the variation of the code phase offset during the dwell time (dynamic case) is considered rather than the static case. Results in the latter case are also indicated for comparison.

Worst-case approach

In this case the signals are assumed received at the same C/N_0 so no improvements in performance are expected between the first and subsequent satellites. If we allocate the probabilities equally between the four events, we have to demonstrate that:

$$\begin{cases} Pb(Acquisition\ time\ 1^{st}\ sat \le 60s) \ge \sqrt[4]{0.95} = 0.987 \approx 0.99 \\ Pb(Acquisition\ time\ next\ sats \le 30s) \ge \sqrt[4]{0.95} = 0.987 \approx 0.99 \end{cases}$$

Then simulations were carried out to compute, given the dwell time, the required numbers of correlators to achieve a probability of acquisition of 0.99 for the first satellite in less than 60 s. Results are indicated in the next figure for various C/N_0 in the "dynamic" case.

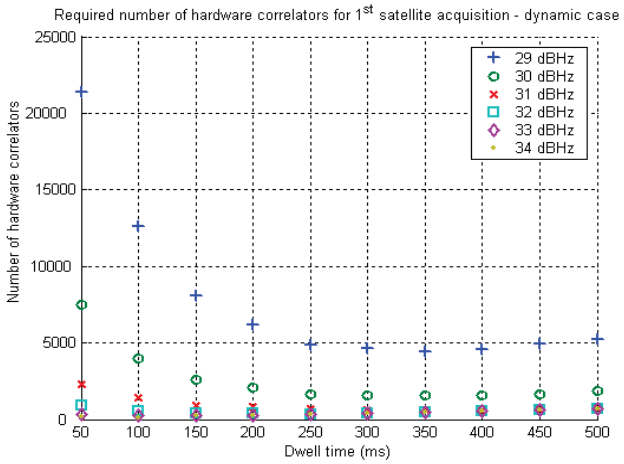

Figure 15 *Required number of hardware correlators vs dwell time for the first satellite acquisition – dynamic case*

Here is a close-up:

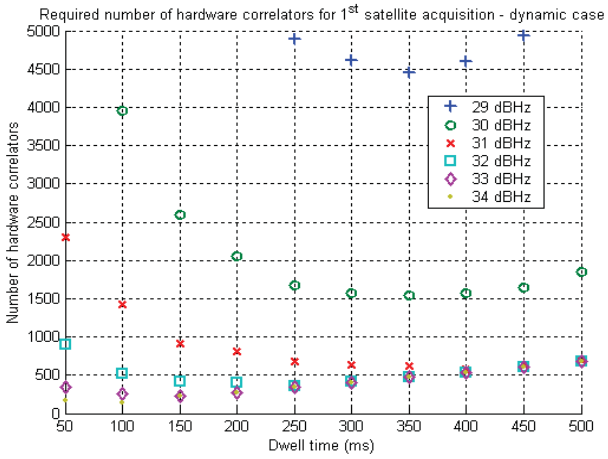

Figure 16 *Close-up - required number of hardware correlators vs dwell time for the first satellite acquisition _ dynamic case*

In the static case, outcomes of simulations are different as shown on the next figure that is a close-up.

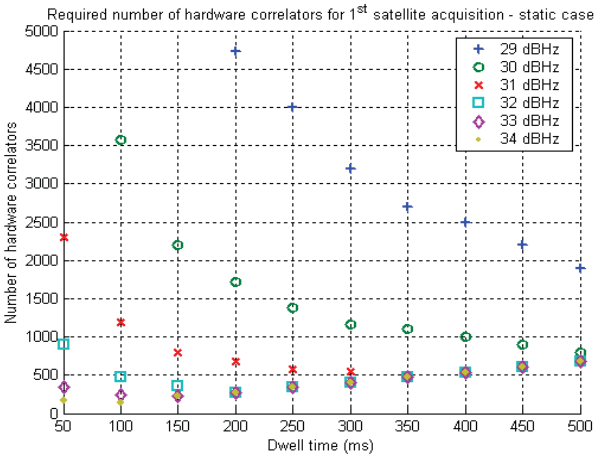

Figure 17 *Close-up - required number of hardware correlators vs dwell time for the first satellite acquisition – static case*

As anticipated from probability of detection plots of Figure 10, the main discrepancies between "static" and "dynamic" cases are observed when the C/N_0 is low and the dwell time is large. For dwell times larger than about 250 ms and C/N_0 of 29 dBHz and 30 dBHz there are substantial differences in the required number of correlators. With these assumptions, the ratio of required correlators ranges from 1.2 to 2.7. When it comes to larger C/N_0, differences are somewhat anecdotic.

For subsequent satellites, we get the following results to perform acquisition in less than 30 seconds with a probability of success of 0.99. First when code phase offset variation is assumed:

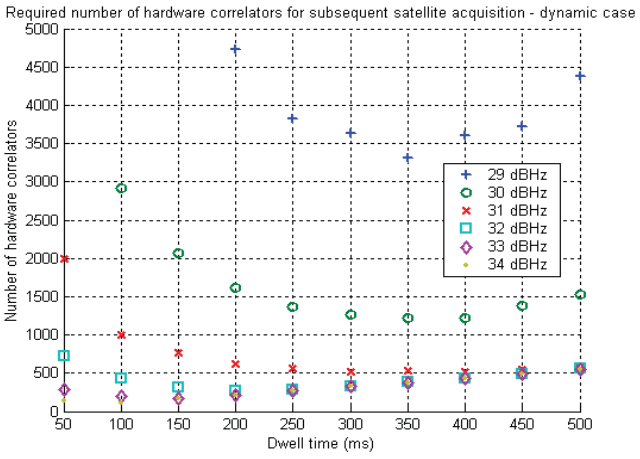

Figure 18 *Close-up - required number of hardware correlators vs dwell time for subsequent satellite acquisition – dynamic case*

In the static case, the required numbers of correlators are different as illustrated in Figure 19 that is again a close-up.

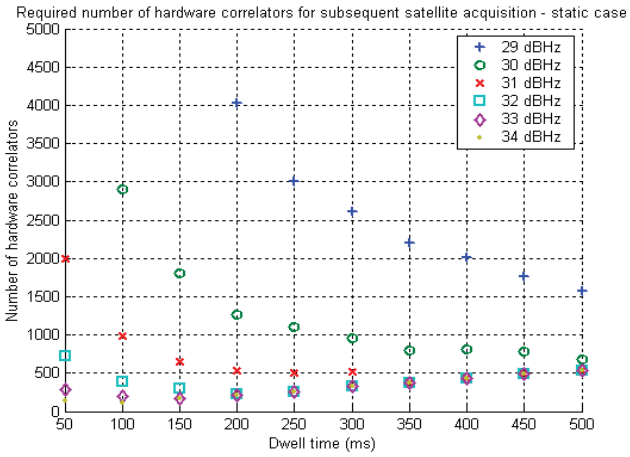

Figure 19 *Close-up - required number of hardware correlators vs dwell time for subsequent satellite acquisition – static case*

For subsequent satellites, the same remarks, as done previously for the first satellite, on differences between "static" and "dynamic" cases can be made. Note also that the required number of correlators is somewhat lower for subsequent satellites. Hence the first satellite acquisition process requirements drive, to a limited extent, the choice of the number of correlators and dwell time.

According to results presented in [10], it is possible to compute the available effective post-correlation C/N_0 for acquisition at high altitude (FL 400) over the EU and US hot-spots. DME/TACAN and JTIDS/MIDS systems are the main interferers at these locations and their impact has been assessed through simulations. Details of simulations can be found in reference [10]. Power link budgets resulting from this study are summarized in the Table 3 for Galileo E5a and E5b, and GPS L5 over the EU hot-spot. Degradations over the EU hot-spot are larger so that if acquisition is possible at this location then it would be the same over the US hot-spot. Inter-system degradations are also accounted for and total interference impact is integrated in the term $N_{o,eff}$ that is the effective noise power spectral density level. Without any interference, $N_{o,eff}$ equates -200 dBW/Hz that is the classical thermal noise PSD level for the considered signals. Note that the antenna gain (-4.5 dBi) is taken at a 5° elevation angle that is assumed to be worst case and that no aeronautical safety margin is added.

From the table, we see the worst case available effective post-correlation C/N_0 equates 29.4 dBHz and corresponds to Galileo E5a.

Note: This figure (29.4 dBHz) considers correlation loss (included in implementation loss of previous table) that is apportioned between useful signal loss $R_f^2(0)$ and thermal

noise power loss β at correlator output. Thermal noise power reduction has already been accounted for when computing performance in previously defined non-centrality parameters. Signal loss, as defined in correlation loss, may be introduced in the generic non-centrality parameter:

$$\lambda = \frac{2}{f_p} \cdot \frac{C}{N_0} \cdot \frac{R_f^2(0)}{\beta} \cdot \left(\frac{\sin(\pi \Delta f T_P)}{\pi \Delta f T_P} \right)^2 \cdot \frac{1}{R_f^2(0)} \cdot \sum_{k=1}^{M} R_f^2(\varepsilon_\tau)$$

Correlation loss are simply $R_f^2(0)/\beta$. Thus, so as to compare available $C/N_{0,eff}$ indicated in Table 3 with C/N_0 used earlier in simulations, a correction must be brought. $R_f^2(0)$ has been estimated to about -1.2 dB. So in order to perform consistent comparison, the available $C/N_{0,eff}$ is 29.4+1.2=30.6 dBHz.

#	Quantity/(units)	Galileo E5a	Galileo E5b	GPS L5
1	Surface Satellite Signal Power (dBW)	-155.0	-155.0	-154.9
2	Implementation loss (dB)	-2.0	-2.5	-2.0
3	Minimum Antenna Gain (dBi)	-4.5	-4.5	-4.5
4	C=recovered SV Power (dBW) (combine logs(1)-(2)+(3)	-161.5	-162.0	-161.4
5	$N_{O,eff}$(dBW/Hz)	-190.9	-192.7	-190.8
6	$C/N_{0,eff}$(subtract (5) from (4)) (dBHz)	29.4	30.7	29.6

Table 3 EU hot-spot Galileo E5a/E5b and GPS L5 power link budget at FL 400

In order to get a positive C/N_0 for acquisition we need to verify whether an acquisition threshold lower than 30.6 dBHz is satisfying. From a worst case perspective, the "dynamic" case is considered. Figure 15 and Figure 16 indicate the associated results for the first satellite acquisition that is the most demanding process. In the light of these figures we see that for a C/N_0 of 30 dBHz and dwell times larger than 150 ms, the required number of hardware correlator is over bounded by about 2500. In the forthcoming years such a number seems reasonable according to avionics manufacturers. This C/N_0 figure is lower than the available effective signal-to-noise density ratio at high altitude (FL 400) over the EU hot-spot for Galileo E5a so feasibility is demonstrated. The number of required correlator may be lowered by increasing the dwell time, the optimal value being 1500 for dwell times in between 300 ms and 350 ms.

SUMMARY AND CONCLUSIONS

We simulated the acquisition process for the single dwell time serial search process. The obtained results are consistent with theoretical derivations available in literature validating our method and model. PRN codes acquisition is performed using both the data and pilot components in order to enhance performance.

A more realistic approach taking into account code phase offset variation over time was considered. The results obtained in this case are pretty different from the classical "static" case where the code phase offset is supposed constant. Differences are particularly pronounced for low C/N_0 and large dwell times. In these cases the required numbers of correlators are larger with a ratio soaring to 2.8 in the worst case. For smaller dwell times, curve slopes are high causing a kind a sensitivity that is not desirable when determining the feasibility of the acquisition requirement.

According to our simulation results, we have demonstrated that an acquisition threshold of about 29 dBHz is achievable with a reasonable number of correlators. Moreover assuming a worst-case approach associated with a worst-case antenna gain, the initial acquisition time requirement of RTCA DO 229 is satisfied for Galileo E5a and E5b and GPS L5 over the EU and US hot spots.

ACKNOWLEDGMENTS

The author would like to express appreciation for the many helpful advises and guidance provided by Eric Chatre from the Galileo Joint Undertaking and Christophe Macabiau from the ENAC. The author would like also to acknowledge the contribution of Hervé Guichon and Nicolas Martin from Thales Avionics France.

REFERENCES

[1] F.Bastide, O.Julien, C.Macabiau, B.Roturier, "Analysis of L5/E5 Acquisition, Tracking and Data Demodulation Thresholds", Proceedings of the Institute of Navigation GPS Meeting, Portland, OR, September 2002

[2] J.K Holmes, *"Coherent Spread Spectrum Systems",* New York, John Wiley & Sons, 1982

[3] F.Bastide, *"Correlation losses expressions"*, ENAC/STNA working note, November 2003

[4] C.Macabiau, L.Ries, F.Bastide, J.L Issler, *"GPS L5 Receiver Implementation Issues"*, Proceedings of the Institute of Navigation GPS Meeting, Portland, OR, September 2002

[5] C.Hegarty, M.Tran, A.J Van Dierendonck, *"Acquisition Algorithms for the GPS L5 Signal"*, Proceedings of the Institute of Navigation GPS Meeting, Portland, OR, September 2003

[6] RTCA SC-159 *"Minimum Operational Performances Standards for Global Positioning System/Wide Area Augmentation System Airborne Equipment"*, RTCA DO 229C

[7] Hegarty, C., T. Kim, S. Ericson, P. Reddan, T. Morrissey, and A.J. Van Dierendonck, *"Methodology for Determining Compatibility of GPS L5 with Existing Systems and Preliminary Results"*, Proceeding of the Institute of Navigation Annual Meeting, Cambridge, MA, June 1999

[8] C.Hegarty, *"Proposed SNR Thresholds for L5 Minimum Operational Performance Standards"*, MITRE document, September 2003

[9] R.J Erlandson, T.Kim, C.Hegarty, A.J Van Dierendonck, *"Pulsed RFI Effects on Aviation Operations Using GPS L5"*, Proceedings of the Institute of Navigation National Technical Meeting, San Diego, CA, January 2004

[10] F.Bastide, E.Chatre, C.Macabiau, *"Galileo E5a/E5b and GPS L5 RFI Assessment Update – Worst Case Power Link Budget over the EU and US Hot-Spots"*, WP 62-9-13, EUROCAE WG 62, Paris, February 2004